Carrier dynamics of the intermediate state in InAs/GaAs quantum dots coupled in a photonic cavity under two-photon excitation

Takashi Kita, Tsuyoshi Maeda, and Yukihiro Harada

Department of Electrical and Electronic Engineering, Graduate School of Engineering, Kobe University, 1-1 Rokkodai, Nada, Kobe 657-8501, Japan

(Received 24 February 2012; revised manuscript received 21 May 2012; published 2 July 2012)

We have studied the time-resolved intraband transition from the intermediate state to the continuum state of the conduction band in InAs/GaAs self-assembled quantum dots (QDs) embedded in a one-dimensional photonic cavity structure using two-color photoexcitation spectroscopy. The resonant energy of the photonic cavity was tuned to enhance the intraband transition with an energy smaller than the interband transition energy between the intermediate state and the quantized hole states. The interband photoluminescence intensity was observed to be drastically reduced due to the pumping out of carriers in the intermediate state using near-infrared laser light. We proposed a model describing the carrier relaxation process in the InAs/GaAs QD system, where the two-photon absorption and the Pauli blocking in QDs are considered.

DOI: 10.1103/PhysRevB.86.035301 PACS number(s): 78.67.Hc, 78.55.Cr, 78.47.jd

I. INTRODUCTION

Intraband transitions in low-dimensional semiconductors have been essential in exploring new concepts in optical devices because of their excellent controllability of infrared transition[1] determined by subband energy spaces, ultrafast response unlimited by carrier recombination lifetime,[2] and optical selection rules.[3] New ideas using intraband transitions can be realized by designing electronic properties of quantized states in low-dimensional structures. In particular, intermediate band solar cell (IBSC) is an attractive concept for the next-generation ultraefficient solar cell because of their extremely high efficiency limit of 63%.[4] By absorbing a sub-band-gap photon, an electron transits from the valence band (VB) to the intermediate band (IB). Upon absorbing another sub-band-gap photon, the electron is further pumped into the conduction band (CB). This process is anticipated to produce extra photocurrent without degrading the photovoltage. Recently, key physical principles needed to understand the responses in IBSCs to multicolor light have been experimentally[5–11] and theoretically[12–17] investigated. When using degenerate quantized states in nanostructures as the IB, the intraband transition efficiency is generally low compared to the interband transition because of the dipole transition selectivity. For example, intraband transitions in two-dimensional quantum wells and superlattices are forbidden for light irradiating along the confinement direction. To improve the probability of the *intraband transition* from IB to CB, we need to introduce much lower-dimensional nanostructures such as quantum dots (QDs)[18–22] and localized impurity states[23,24] when sunlight illuminates the solar cell surface along the normal direction. A great deal of effort has been put into the investigation of the photoexcitation mechanism in IBSC using InAs self-assembled QDs. However, conventional InAs self-assembled QDs have a lenslike form, and its strong vertical confinement leads energy states very similar to a quantum well which give rise to less sensitivity to light coming from the vertical direction.

Recently, we performed numerical simulations regarding the effects of absorption coefficients on the IB configuration in InAs/GaAs QD-IBSCs.[15] In this case, when the ratio of the absorption coefficients between the transitions of IB-CB and VB-IB, α_{IC}/α_{VI}, is decreased, increasing the IB levels increases the photon flux from the IB to the CB and decreases the photon flux from the VB to the IB, which eventually compensates for the decrease in the α_{IC}/α_{VI}.[15] The optimum E_{VI} level depends on α_{IC}/α_{VI}. Overall, a large α_{IC} is necessary for high conversion efficiency, because of the relatively low photon flux in the infrared region of the solar spectrum.

To effectively enhance the intraband transition, we focus on photonic cavity structures. Figure 1 is a schematic diagram of the photoexcitation of carriers and the relaxation processes in a semiconductor with a single intermediate band. Two-color photoexcitation has been carried out by using a continuous wave (cw) laser light for the interband transition and near-infrared (NIR), pulsed laser light to excite the intermediate state. The cavity can dramatically enhance the interaction between the electronic states in QDs and light. By controlling the resonant wavelength of the photonic cavity, we can selectively improve the intraband transition. In this study, we demonstrate carrier excitation and relaxation processes in the intermediate state of InAs/GaAs self-assembled QDs using two-color photoexcitation spectroscopy. In particular, the effects of a photonic cavity enhancing carrier excitation in the intermediate state are discussed.

II. FABRICATION OF QUANTUM DOTS IN PHOTONIC CAVITY

Figure 2(a) is a schematic diagram of a photonic cavity structure fabricated on GaAs(001) by solid-source molecular beam epitaxy. The λ cavity includes two distributed Bragg reflector (DBR) mirrors; the λ cavity layer (376.8 nm) was sandwiched in between top and bottom mirrors consisting of alternative GaAs and AlAs layers each of which has a film thickness of $\lambda/4$. The periods of the top and bottom mirrors were 5 and 9, respectively. The total thicknesses of the top and bottom mirror layers are 1028.5 and 1851.3 nm, respectively. The DBR mirrors were grown at 500 °C. Three QD layers were inserted into the antinode portion of the electromagnetic field to enhance the interaction between the

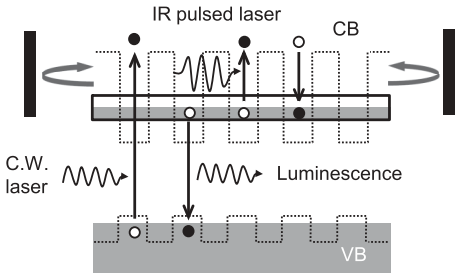

FIG. 1. Schematic diagram of photoexcitation of carriers and relaxation processes in a semiconductor with a single intermediate band. Two-color photoexcitation has been carried out by using a continuous wave laser light for the interband transition and near-infrared, pulsed laser light to excite the intermediate state. This figure illustrates a diagram just after the pulse excitation. Excited electrons and holes are indicated schematically by closed and open circles. The cavity can dramatically enhance the interaction between the electronic states in QDs and light.

QD and light. The positions of the QD layers are indicated by dotted lines in Fig. 2(a). InAs QDs were formed by depositing 2.4 ML of InAs at 480 °C. The thickness of the GaAs spacer layer between the QD layers was 50 nm. The 50-nm GaAs spacer layer is thick enough to separate the QD layers, and thus the electronic coupling between QDs stacked along the growth direction is negligible. Recently, we have performed transmission electron microscopy and an electron tomography for embedded InAs/GaAs QDs grown at the same conditions. The QD was confirmed to be slightly elongated along the [−110] crystal axis. The average QD height was ∼5 nm, and the base lengths are approximately 21 and 23 nm along [110] and [−110], respectively.[25,26] The QD density was $\sim 4 \times 10^{10}$ cm^{-2}, which roughly corresponds to the average in-plane interdot spacing of approximately 50 nm. Furthermore, we provided a reference sample with the three InAs QD layers without the cavity structure. The QDs were grown by the same conditions.

A normal reflectivity spectrum of the cavity structure measured at room temperature is shown in Fig. 2(b) and is compared with a spectrum calculated numerically using a transfer matrix method. The resonant wavelength was 1300 nm and the measured Q value of this cavity was 77. It should be noted that the resonant wavelength varies as a function of the incident angle of light. The resonant wavelengths measured at different incident angles are indicated in Fig. 2(c). The resonant position shifts approximately 60 nm as the incident angle is increased by 60°. When using a concentrator photovoltaic cell, such an angle-dependent broadband optical response is essential.

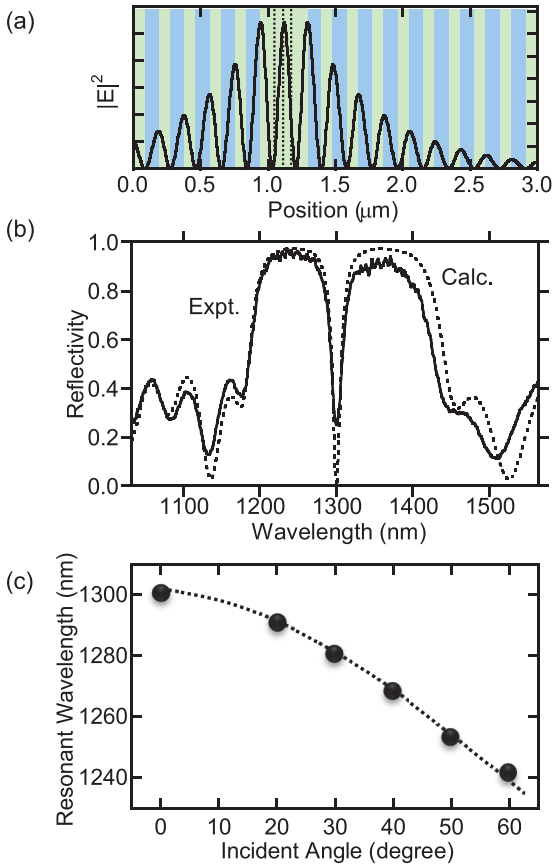

FIG. 2. (Color online) (a) Schematic illustration for the designed structure of a one-dimensional photonic cavity including three QD layers. The λ cavity includes two distributed Bragg reflector mirrors, which consist of alternative GaAs and AlAs layers each of which has a film thickness of λ/4. The periods of the top and bottom mirrors were 5 and 9, respectively. QD layers are inserted into the antinode portion of the electromagnetic field to enhance the interaction between the QD and light. (b) Measured and calculated cavity reflectivities at room temperature. (c) Incident angle dependence of the resonant wavelength. The resonant position shifts approximately 60 nm as the angle is increased by 60°.

III. TWO-COLOR PHOTOEXCITATION SPECTROSCOPY

Two-color photoexcitation spectroscopy was carried out at 4 K using a near-infrared streak-camera system. A cw laser light with a wavelength of 659 nm irradiated the sample to create carriers in the QD system. In Fig. 1, excited electrons and holes are indicated schematically by closed and open circles. In the steady state, the carrier density of the intermediate state is determined by the cw-carrier generation and the radiative recombination rate. The intermediate state was selectively excited using NIR, pulsed laser light. The pulsed light source used was generated by an optical parametric oscillator (OPO) excited by a mode-locked Ti:sapphire laser. The pulse duration was approximately 200 fs and the repetition rate was 80 MHz. The wavelength of 1300 nm was chosen to excite at the resonant wavelength of the cavity, which was precisely determined by confirming the resonance structure that appeared in the reflection spectrum of the 200 fs broadband pulse. The laser beam diameter of both the cw- and pulse-excitation lasers at the sample surface was 300 μm. In this study, we observed streak-camera images of the photoluminescence (PL) created by the cw laser light. Here, we refer to the interband transition in QDs. The interband PL intensity is changed according to a change in the carrier density of the intermediate state that is modulated by the ultrafast IR laser pulse excitation.

IV. RESULTS AND DISCUSSION

A. Two-color photoexcitation spectrum and enhanced intraband transition in photonic cavity

First, we confirmed the interband transition wavelength being shorter than the pulse-excitation wavelength. Since the cavity resonant feature also changes the PL line shape observed from the surface, we measured PL of the reference sample without the cavity structure. Figure 3 displays the excitation power dependence of PL spectra of the reference sample. The measurement was carried out at 17 K. With the increase in the excitation power, PL signals from the excited states become clear. The peak wavelength of the PL is approximately 1140 nm, which is shorter than 1300 nm of the pulse-excitation wavelength as indicated in this figure. In the two-color photoexcitation spectroscopy performed at 4 K, the laser pulses exciting the sample pass through the fundamental interband optical gap without being absorbed. The energy difference between the PL peak and the GaAs band gap is approximately 0.39 eV, which is smaller than the photon energy (0.95 eV) of the 1300 nm excitation pulse laser light. Thus, the cavity can selectively enhance the intraband transition from the intermediate state to the continuum state located above the conduction-band edge. The final level is 0.56 eV from the conduction-band edge.

Typical results of the two-color photoexcitation spectroscopy are shown in Fig. 4. Here, we indicate the PL intensity integrated in the whole spectrum. The cw-excitation power was 1 mW, and the pulse-excitation power was varied. The PL intensity decreased abruptly immediately after the excitation. The dip structure in the PL response was followed by a gain, which is direct evidence of carrier excitation from the intermediate state and the following relaxation into the initial state. This PL-intensity reduction means that radiative recombination loss was reduced. As the pulse-excitation power was increased, the reduction in PL intensity increased and eventually exceeded 60%. When the intermediate state is excited by the pulsed laser light, the carrier density of the intermediate state decreases and radiative recombination will

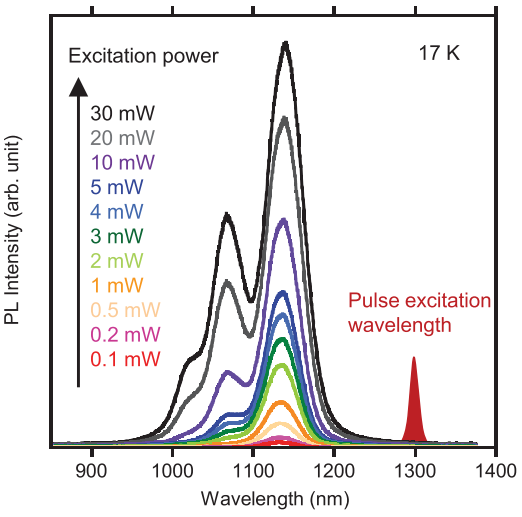

FIG. 3. (Color online) Excitation power dependence of PL spectra of the reference sample. The measurement was carried out at 17 K.

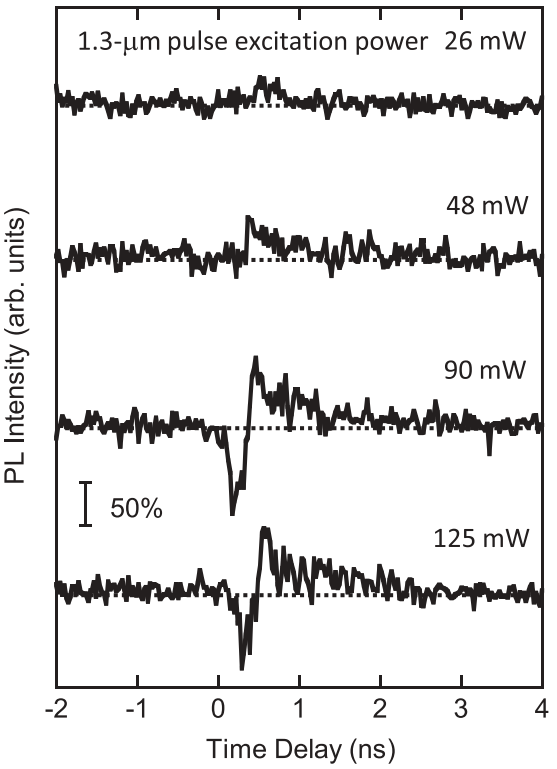

FIG. 4. Two-color excitation signal measured at 4 K. PL intensity was integrated in the whole spectrum. The cw-excitation power was 1 mW, and the pulse-excitation power was varied. The PL intensity decreased abruptly immediately after the excitation. The dip structure in the PL response was followed by a gain. The bar indicates the amplitude corresponding to a 50% change of the signal.

therefore be reduced. This would be observed by a change in the PL intensity. A similar decrease of the PL at the interband transition has previously been observed in InAs/GaAs QDs by Murdin *et al.*[27] They performed double resonance spectroscopy using a cw HeNe laser for interband excitation and a far-infrared free electron laser for bound-to-bound intraband transition. A decrease of the PL for the fundamental interband transition and an increase for higher transitions was observed through a population transfer from the ground state to higher energy states. Our results demonstrate that the *bound-to-free* intraband transition also causes a modulation of the PL.

Figure 5 compares the fraction of the PL-intensity reduction observed for QDs with and without the cavity structure. Figures 5(a) and 5(b) show results obtained at cw-excitation powers of 1.0 and 0.25 mW, respectively. The maximum fraction of the PL-intensity reduction is indicated in Fig. 5. The PL-intensity reduction becomes significant when using QDs with the cavity structure. The dependence of the reduction in PL intensity on the excitation pulse power behaves linearly as indicated by the lines. Using the cavity structure, the signal amplitude increases by a factor of 8. This means the interaction between QDs and light in the cavity structure is enhanced. However, the enhancement caused by the cavity structure is smaller than that expected from the Q value. As shown in Fig. 2(b), the cavity allows the incident light to pass through within the narrow spectral range of $\Delta\lambda \sim 14$ nm. This extremely narrow bandpass filter feature decreases the

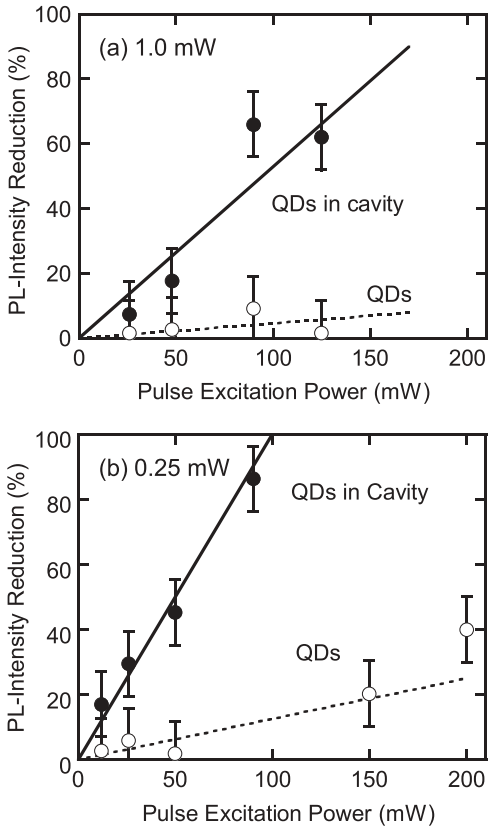

FIG. 5. Pulse-excitation power dependence of the maximum PL-intensity reduction for QDs with (closed circles) and without (open circles) the cavity structure. (a) and (b) show results obtained at cw-excitation powers of 1.0 and 0.25 mW, respectively. The maximum fraction of the PL-intensity reduction measured at the time the dip was observed is indicated here. Solid and dashed lines guide linear relations.

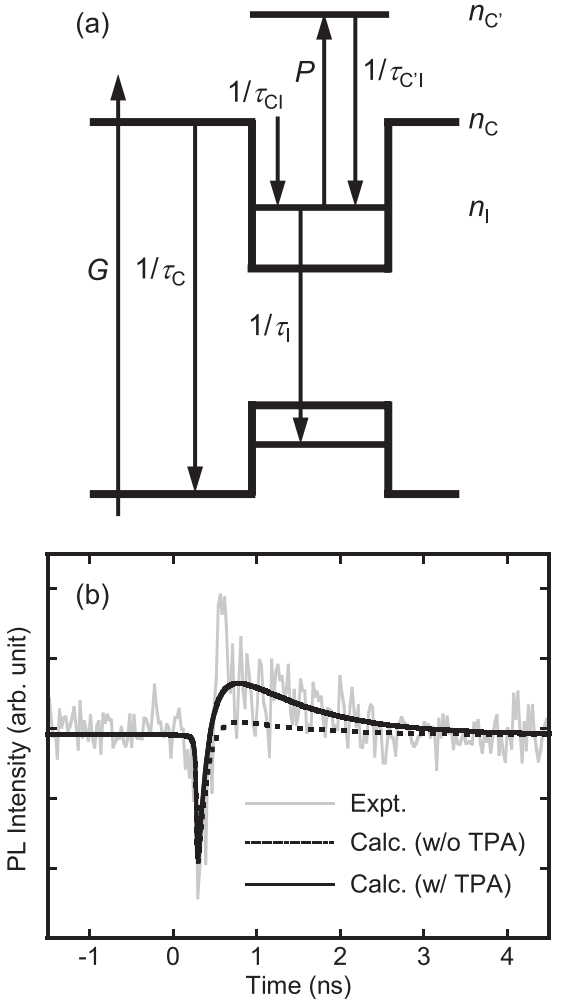

FIG. 6. (a) Three-level model representing excitation and relaxation processes. (b) Gray solid and black dotted lines indicate experimental and theoretical responses of PL intensity created by a pulse excitation, respectively. The experimental data was measured at cw-excitation power of 1 mW and pulse-excitation power of 125 mW. The theoretical response was calculated at a $\tau_{C'I}$ of 0.1 ns. The black solid line indicates the theoretical response including the two-photon absorption process at $\tau_{C'I}$ of 0.1 ns and N_{TPA} of $\sim 0.36 \times N_P$.

excitation intensity by approximately a quarter. Since the Q value is 77, the quarter excitation intensity is presumed to assure an amplification of the signal of approximately 19. But the observed factor of the amplification was 8. Such discrepancy may arise from saturable absorption under the strong pulse excitation in QDs because of the low density of the intermediate states.

The PL-intensity reduction depends on the cw-excitation power. The low cw-excitation power causes a dramatic reduction in the PL intensity. A strong pumping power is essential to sufficiently excite the intermediate state. Moreover, the low transition probability of the intraband transition and the low confinement factor of QDs give rise to several demands for efficient excitation of the intermediate state. Next, we discuss the excitation and relaxation process.

B. Carrier dynamics of the intraband excitation and relaxation in InAs/GaAs QDs

After pumping out carriers from the intermediate state into the conduction band, the excited carriers relax again to the initial state. The excess carriers lead to an increase in the PL intensity according to the change in the carrier density of the intermediate state as shown in Fig. 4. The amplitude of the gain is also proportional to the reduction in the PL intensity. Figure 6(a) illustrates a model that can assist the interpretation of the observed results. The cw laser excites the valence-band electrons to the conduction band at the rate of G. The populated electron density in the conduction band is n_C. The excited electrons relax to the intermediate state and the valence band with time constants of τ_{CI} and τ_C, respectively. The electron density of the intermediate state is n_I. Electrons in the intermediate state recombine with a time constant of τ_I in radiative and nonradiative processes. The IR laser pulse excites electrons in the intermediate state to the conduction band. Here, we assumed that the electrons excited by the IR laser pulse do not relax to the valence band because holes are not created. The electron density excited by the IR laser pulse in the conduction band is $n_{C'}$, which relaxes to the intermediate state with a time constant of $\tau_{C'I}$. The excitation rate by the IR laser, P, is expected to be proportional to the laser

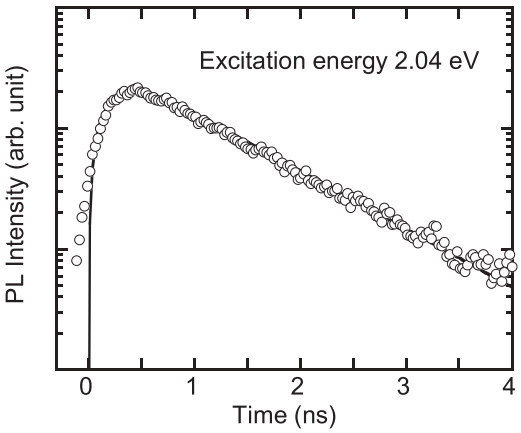

FIG. 7. PL-decay curve measured at 4 K. The PL intensity was integrated in the whole spectrum. The excitation energy was 2.04 eV.

amplitude. The sech^2-shaped function was used to represent the excitation pulse shape at a time of t_0. The full width at half maximum of the laser pulse is approximately $1.76 \times \Delta$, where Δ is the pulse duration appearing in the sech^2-shaped function as shown in the following equations. The excited electron number per pulse is N_P. Using these parameters, the following phenomenological rate equations can be derived.

$$\frac{dn_{\mathrm{C}}(t)}{dt} = G - \frac{n_{\mathrm{C}}(t)}{\tau_{\mathrm{CI}}}\left(1 - \frac{n_{\mathrm{I}}(t)}{2}\right) - \frac{n_{\mathrm{C}}(t)}{\tau_{\mathrm{C}}}, \tag{1}$$

$$\frac{dn_{\mathrm{C}'}(t)}{dt} = -\frac{n_{\mathrm{C}'}(t)}{\tau_{\mathrm{C}'\mathrm{I}}}\left(1 - \frac{n_{\mathrm{I}}(t)}{2}\right) + P, \tag{2}$$

$$\frac{dn_{\mathrm{I}}(t)}{dt} = \frac{n_{\mathrm{C}}(t)}{\tau_{\mathrm{CI}}}\left(1 - \frac{n_{\mathrm{I}}(t)}{2}\right) + \frac{n_{\mathrm{C}'}(t)}{\tau_{\mathrm{C}'\mathrm{I}}}\left(1 - \frac{n_{\mathrm{I}}(t)}{2}\right) - \frac{n_{\mathrm{I}}(t)}{\tau_{\mathrm{I}}} - P, \tag{3}$$

$$P = \frac{N_P}{2\Delta}\mathrm{sech}^2\left(\frac{t - t_0}{\Delta}\right). \tag{4}$$

Here, the first and second terms of Eq. (3) represent carrier injection from GaAs (n_{C}) and energy relaxation from the extended states with a high energy in QDs ($n_{\mathrm{C}'}$), respectively. These equations include the Pauli blocking factor $1 - n_{\mathrm{I}}/2$ for the intermediate state, which is satisfied when N_P is not larger than n_{I} at the steady state. In this study, we assumed that N_P is equal to the steady-state value of n_{I} because saturable absorption was expected to be observed as discussed above. On the other hand, the carrier generation rate G by the cw laser should be low according to the experimental excitation power of 1 mW so that the effect of the Pauli blocking is considered to be negligible. We assumed that the carrier relaxation rate τ_{CI} is constant. The recombination time in the GaAs conduction band, τ_{c}, was assumed to be 3.3 ns, which corresponds to the radiative lifetime of free excitons in GaAs.[28] In this work, we estimated τ_{CI} and τ_{I} from the time-resolved PL dynamics.[29] The open circles in Fig. 7 indicate a spectrally integrated PL-decay profile measured at 4 K. A frequency doubler of the OPO was used for the excitation; the excitation energy was 2.04 eV and the pulse duration was approximately 200 fs. The energy difference between the excitation light and the GaAs band edge of 1.51 eV was 0.53 eV. The solid line in Fig. 7 shows a theoretical result. Since the sample temperature during the measurement was 4 K, we can neglect effects of in-plane interdot carrier transfer on the rise time. Therefore, τ_{CI} is considered to correspond to the rise time of the PL intensity increasing immediately after the excitation if the carrier relaxation is mostly limited by the relaxation of electrons. On the other hand, τ_{I} is given by the decay time. The obtained τ_{CI} and τ_{I} were 0.3 and 0.9 ns, respectively.

Using these values, we calculated the PL response according to the temporal dependence of n_{I}, which is broadened by convolution with a Lorentzian with a full width at half maximum of 20 ps, which is the resolution of our streak-camera system. The gray solid and black dotted lines in Fig. 6(b) indicate the experimental and theoretical responses of the PL intensity created by a pulsed excitation. The experimental data was measured at a cw-excitation power of 1 mW and a pulse-excitation power of 125 mW, and the theoretical response was calculated at a $\tau_{\mathrm{C}'\mathrm{I}}$ of 0.1 ns. The carrier generation rate G used in this calculation was 0.1 ns^{-1}. The calculated PL response reproduces the observed dip structure followed by the gain. However, the calculated amplitude of the gain is very small and cannot interpret the experimental observation. Recently, a similar dip structure followed by a gain has been observed in a spectrally resolved PL response in InAs/GaAs QDs, which has been considered to be caused by redistribution of carriers into the neighboring QDs after the bound-to-bound intraband transition excited by a far-infrared free electron laser.[30] Although the carrier redistribution is one of the possible origins of such significant gain, this is unlikely in our case because we detected the spectrally integrated PL response. Another possible origin of the significant gain is an increased carrier density in the GaAs (n_{C}) by the two-photon absorption process. In order to clarify the effects of the two-photon absorption, we added a term $(N_{\mathrm{TPA}}/2\Delta)\mathrm{sech}^2\{(t - t_0)/\Delta\}$ in Eq. (1). Here, N_{TPA} is the excited electron number per pulse by the two-photon absorption process. The black solid line in Fig. 6(b) indicates the calculated PL response at a $\tau_{\mathrm{C}'\mathrm{I}}$ of 0.1 ns and a N_{TPA} of approximately $0.36 \times N_P$. This value of N_{TPA} is considered to be an acceptable value according to the well-known two-photon absorption coefficient of GaAs.[31] The calculated PL response including the two-photon absorption process reproduces the observed result. In particular, the relatively slow temporal response of the gain agrees well with the calculation, which is a unique feature of our result. Extra electrons created by the two-photon absorption process relax into the intermediate state of QD and recombine with holes with τ_{I}. Thus, τ_{I} limits the temporal evolution. Since τ_{I} is 0.9 ns, the temporal change of the gain signal is slow as compared with the PL-intensity reduction at $t - t_0 = 0$. This result suggests that the observed PL response results from both the bound-to-free intraband transition and the increased carrier density in GaAs created by the IR laser pulse excitation.

The amplitudes of both the PL-intensity reduction and gain increase with the increase in the N_P. On the other hand, as shown in Fig. 5, the signal amplitude has been observed to depend on the cw-excitation power; the amplitude increases with decreasing the cw-excitation power. In our model, the cw-excitation power corresponds to G. We confirmed that the temporal evolution of n_{I} also depends on G. According to

our calculations, the relative amplitude of the dip at $t - t_0 = 0$, $1 - n_{\mathrm{I,dip}}/n_{\mathrm{I,steady}}$, decreases with increasing G when the N_P is fixed. This indicates that rapid carrier relaxation from GaAs into QDs can compensate the reduction in n_{I}, which becomes remarkable with G. In particular, the $1 - n_{\mathrm{I,dip}}/n_{\mathrm{I,steady}}$ was remarkably decreased when the effect of the Pauli blocking could not be ignored at large G values, because the carrier relaxation from GaAs into QDs is increased due to the high carrier density in the GaAs barrier region. Furthermore, our calculations predict that the reduction of n_{I} at $t - t_0 = 0$ becomes fast and the gain disappears with increasing G, whereas both the dip and gain structures are very clear at low G.

V. SUMMARY

The carrier dynamics in the intermediate state of InAs/GaAs self-assembled QDs embedded in a one-dimensional photonic cavity structure has been studied by using two-color photoexcitation spectroscopy. The fundamental radiative recombination from the intermediate state to the quantized hole states was found to be reduced by pumping out carriers from the intermediate state; the PL intensity abruptly decreases just after the excitation. The dip structure in the PL response is followed by a gain, which is direct evidence of carrier excitation from the intermediate state and the following relaxation into the initial state. The gain signal shows a slow temporal response. The change in the interband PL intensity increases with the power of the excitation pulse. The photonic cavity selectively enhances the intraband transition, and the PL response was observed to increase by a factor of 8. To interpret the results, we proposed a model describing the carrier relaxation process in the InAs/GaAs QD system, where the two-photon absorption and the Pauli blocking in QDs are considered. According to these calculations, the observed PL response results from both the bound-to-free intraband transition and the increased carrier density in GaAs created by the two-photon absorption of the IR laser pulse excitation.

ACKNOWLEDGMENTS

We would like to thank O. Kojima of Kobe University for fruitful discussions. This work was partially supported by the Scientific Research Grant-in-Aid from the Ministry of Education, Culture, Sports, Science and Technology (MEXT) (Grants No. 22241035 and No. 21360151), the Incorporated Administrative Agency New Energy and Industrial Technology Development Organization (NEDO), and Ministry of Economy, Trade and Industry (METI), Japan.

[1] M. Helm, P. England, E. Colas, F. DeRosa, and S. J. Allen Jr., Phys. Rev. Lett. **63**, 74 (1989).
[2] *Femtosecond Technology: From Basic Research to Application Prospects*, edited by T. Kamiya, F. Saito, O. Wada, H. Yajima (Springer-Verlag, Berlin, 1999).
[3] S. Maimon, E. Finkman, G. Bahir, S. E. Schacham, J. M. Garcia, and P. M. Petroff, Appl. Phys. Lett. **73**, 2003 (1998).
[4] A. Luque and A. Martí, Phys. Rev. Lett. **78**, 5014 (1997).
[5] A. Luque, A. Martí, N. López, E. Antolín, E. Cánovas, C. Stanley, C. Farmer, L. J. Caballero, L. Cuadra, and J. L. Balenzategui, Appl. Phys. Lett. **87**, 083505 (2005).
[6] A. Martí, E. Antolín, C. R. Stanley, C. D. Farmer, N. López, P. Díaz, E. Cánovas, P. G. Linares, and A. Luque, Phys. Rev. Lett. **97**, 247701 (2006).
[7] A. Martí, N. López, E. Antolín, E. Cánovas, A. Luque, C. R. Stanley, C. D. Farmer, and P. Díaz, Appl. Phys. Lett. **90**, 233510 (2007).
[8] R. Oshima, A. Takata, and Y. Okada, Appl. Phys. Lett. **93**, 083111 (2008).
[9] Y. Okada, R. Oshima, and A. Takata, J. Appl. Phys. **106**, 024306 (2009).
[10] E. Antolín, A. Martí, C. D. Farmer, P. G. Linares, E. Hernández, A. M. Sánchez, T. Ben, S. I. Molina, C. R. Stanley, and A. Luque, J. Appl. Phys. **108**, 064513 (2010).
[11] Y. Okada, T. Morioka, K. Yoshida, R. Oshima, Y. Shoji, T. Inoue, and T. Kita, J. Appl. Phys. **109**, 024301 (2011).
[12] A. Luque, A. Martí, N. López, E. Antolín, E. Cánovas, C. Stanley, C. Farmer, and P. Díaz, J. Appl. Phys. **99**, 094503 (2006).
[13] A. Luque, P. G. Linares, E. Antolín, E. Cánovas, C. D. Farmer, C. R. Stanley, and A. Martí, Appl. Phys. Lett. **96**, 013501 (2010).
[14] K. Yoshida, Y. Okada, and N. Sano, Appl. Phys. Lett. **97**, 133503 (2010).
[15] W. G. Hu, T. Inoue, O. Kojima, and T. Kita, Appl. Phys. Lett. **97**, 193106 (2010).
[16] W. G. Hu, Y. Harada, A. Hasegawa, T. Inoue, O. Kojima, and T. Kita, Prog. Photovoltaics, doi:10.1002/pip.1208.
[17] P. G. Linares, A. Martí, E. Antolín, and A. Luque, J. Appl. Phys. **109**, 014313 (2011).
[18] S. Tomić, T. S. Jones, and N. M. Harrison, Appl. Phys. Lett. **93**, 263105 (2008).
[19] S. Tomić, Phys. Rev. B **82**, 195321 (2010).
[20] S. Tomić, A. Martí, E. Antolín, and A. Luque, Appl. Phys. Lett. **99**, 053504 (2011).
[21] M. Usman, T. Inoue, Y. Harada, G. Klimeck, and T. Kita, Phys. Rev. B **84**, 115321 (2011).
[22] Y. Ikeuchi, T. Inoue, M. Asada, Y. Harada, T. Kita, E. Taguchi, and H. Yasuda, Appl. Phys. Express **4**, 062001 (2011).
[23] C. Tablero, A. Martí, and A. Luque, Appl. Phys. Lett. **96**, 121104 (2010).
[24] N. López, L. A. Reichertz, K. M. Yu, K. Campman, and W. Walukiewicz, Phys. Rev. Lett. **106**, 028701 (2011).
[25] T. Kita, T. Inoue, O. Wada, M. Konno, T. Yaguchi, and T. Kamino, Appl. Phys. Lett. **90**, 041911 (2007).
[26] T. Inoue, T. Kita, O. Wada, M. Konno, T. Yaguchi, and T. Kamino, Appl. Phys. Lett. **92**, 031902 (2008).
[27] B. N. Murdin, A. R. Hollingworth, J. A. Barker, D. G. Clarke, P. C. Findlay, C. R. Pidgeon, J.-P. R. Wells, I. V. Bradley, S. Malik, and R. Murray, Phys. Rev. B **62**, R7755 (2000).

[28]G. W. p't Hooft, W. A. J. A. van der Poel, L. W. Molenkamp, and C. T. Foxon, Phys. Rev. B **35**, 8281 (1987).

[29]F. Adler, M. Geiger, A. Bauknecht, F. Scholz, H. Schweizer, M. H. Pilkuhn, B. Ohnesorge, and A. Forchel, J. Appl. Phys. **80**, 4019 (1996).

[30]J. Bhattacharyya, S. Zybell, S. Winnerl, M. Helm, M. Hopkinson, L. R. Wilson, and H. Schneider, Appl. Phys. Lett. **100**, 152101 (2012).

[31]D. A. Kleinman, Robert C. Miller, and W. A. Nordland, Appl. Phys. Lett. **23**, 243 (1973).